Elsevier Editorial System(tm) for Clinical Neurophysiology

Manuscript Draft

Manuscript Number: CLINPH-D-13-6764

Title: Improving the reliability of automatically detected dynamic interburst intervals in neonates with hypoxic ischemic encephalopathy

Article Type: Full Length Article

Section/Category: Technical/methodological contributions

Keywords: automated interburst interval detection; grading background EEG; perinatal asphyxia; EEG discontinuity; automated EEG analysis.

Corresponding Author: Mr. Vladimir Matic,

Corresponding Author's Institution: KU Leuven

First Author: Vladimir Matic

Order of Authors: Vladimir Matic; Perumpillichira J Cherian; Katrien Jansen; Ninah Koolen; Gunnar Naulaers; Renate M Swarte; Paul Govaert; Sabine Van Huffel; Maarten De Vos

Suggested Reviewers: Sampsa Vanhatalo Dr. MD PhD
Dept clin neurophysiology, Children's Castle hospital, Helsinki, Finlnad
sampsa.vanhatalo@helsinki.fi

Magnus Thordstein Dr. MD PhD
Institute of Neuroscience and Physiology, Sahlgrenska Academy, Sahlgrenska University Hospital, Göteborg, Sweden
Magnus.Thordstein@neuro.gu.se

Perrine Plouin Dr.
Clinical Neurophysiologist, Hôpital necker Enfants Malades, Paris, France
perrine.plouin@nck.aphp.fr

Warren T Blume Prof., MD, FRCP(C)
Department of Clinical Neurological Sciences, London Health Sciences Centre, Ontario, Canada
Warren.Blume@lhsc.on.ca

Opposed Reviewers:

Abstract:

Objective: to develop an automated system (*NeoGuard_B*) for the reliable selection of certain *dynamic* interburst intervals (*dIBIs*) from all detected *dIBI* candidates (*NeoGuard_A*).

Methods: First, all detected *dIBIs* are classified visually into two subsets: *definite* or *misclassified*. Next, a set of reliability parameters (features) is calculated for each detected *dIBI*. These reliability parameters are used as input feature vectors to four classifiers (LS-SVM) with the objective of distinguishing *definite dIBIs* from *uncertain* detections.

***Results*:** 1h continuous EEG (cEEG) segments from 38 term neonates with postasphyxial encephalopathy were processed. In total, 4408 detected *dIBI* candidates were visually classified as: *definite* (2273) or *misclassified* (2135). Next, the performance of the improved system (*NeoGuard_B*) was tested on cEEG segments, of 30 minutes each, selected from a new dataset of 8 neonates. For all classifiers, significantly improved good detection rates are achieved (compared to *NeoGuard_A*): 98% (68%), 97% (77%), 88% (75%) and 95% (57%). Moreover, we analyzed 152 cEEG segments of 2h duration from 38 neonates (four per neonate). Median duration and amplitude of *dIBIs* within cEEG epochs showed high correlation with visually assessed background EEG grades.

Conclusion: *NeoGuard_B* accurately detects *definite dIBIs* and discards *misclassifications* caused by artifacts, neonatal epileptic seizures or ambiguous EEG patterns, thereby refining the performance of the algorithm.

Significance: *NeoGuard* (*A+B*) reliably classifies background EEG discontinuities, making it suited for automated monitoring of brain dysfunction in the NICU.

*Manuscript
Click here to view linked References

Improving the reliability of automatically detected *dynamic* interburst intervals in neonates with hypoxic ischemic encephalopathy

Vladimir Matic[a,b], Perumpillichira J Cherian[c], Katrien Jansen[d], Ninah Koolen[a,b], Gunnar Naulaers[e], Renate M Swarte[f], Paul Govaert[f], Sabine Van Huffel[a,b], Maarten De Vos[g,a]

[a]KU Leuven, Department of Electrical Engineering-ESAT, SCD-SISTA, Leuven, Belgium

[b]iMINDs Future Health Department

[c]Section of Clinical Neurophysiology, Department of Neurology, Erasmus MC, University Medical Center, Rotterdam, The Netherlands

[d]Department of Pediatrics, University Hospital Gasthuisberg, Leuven, Belgium.

[e]Neonatal Intensive Care Unit, University Hospital Gasthuisberg, Leuven, Belgium.

[f]Section of Neonatology, Department of Pediatrics, Erasmus MC-Sophia Children's Hospital, University Medical Center, Rotterdam, The Netherlands

[g]Neuropsychology Lab, Department of Psychology, University of Oldenburg, Oldenburg, Germany

Address for correspondence:

Vladimir Matic
KU LEUVEN/ESAT/SCD/SISTA
Kasteelpark Arenberg 10, bus 2446
3001 Heverlee, BELGIUM
Tel: +32 16/321085
Email: Vladimir.Matic@esat.kuleuven.be

Key words: automated interburst interval detection; grading background EEG; perinatal asphyxia; EEG discontinuity; automated EEG analysis.

Financial Support: V.M. is supported by a Research Council KUL: GOA MaNet, PFV/10/002 (OPTEC); Flemish Government: IWT: TBM110697-NeoGuard; iMinds 2013.

Highlights

- *Dynamic* interburst intervals (*dIBIs*) are post-processed, thereby improving the detection certainty of EEG discontinuities in neonates with HIE.
- Developed framework of reliability parameters quantifies *dIBIs* detection certainty.
- Median duration and amplitude of *dIBIs* can predict the background EEG abnormalities.

Abstract:

Objective: to develop an automated system (*NeoGuard_B*) for the reliable selection of certain *dynamic* interburst intervals (*dIBIs*) from all detected *dIBI* candidates (*NeoGuard_A*).

Methods: First, all detected *dIBIs* are classified visually into two subsets: *definite* or *misclassified*. Next, a set of reliability parameters (features) is calculated for each detected *dIBI*. These reliability parameters are used as input feature vectors to four classifiers (LS-SVM) with the objective of distinguishing *definite dIBIs* from *uncertain* detections.

***Results*:** 1h continuous EEG (cEEG) segments from 38 term neonates with postasphyxial encephalopathy were processed. In total, 4408 detected *dIBI* candidates were visually classified as: *definite* (2273) or *misclassified* (2135). Next, the performance of the improved system (*NeoGuard_B*) was tested on cEEG segments, of 30 minutes each, selected from a new dataset of 8 neonates. For all classifiers, significantly improved good detection rates are achieved (compared to *NeoGuard_A*): 98% (68%), 97% (77%), 88% (75%) and 95% (57%). Moreover, we analyzed 152 cEEG segments of 2h duration from 38 neonates (four per neonate). Median duration and amplitude of *dIBIs* within cEEG epochs showed high correlation with visually assessed background EEG grades.

Conclusion: *NeoGuard_B* accurately detects *definite dIBIs* and discards *misclassifications* caused by artifacts, neonatal epileptic seizures or ambiguous EEG patterns, thereby refining the performance of the algorithm.

Significance: *NeoGuard* (*A+B*) reliably classifies background EEG discontinuities, making it suited for automated monitoring of brain dysfunction in the NICU.

1. Introduction

In neonatal intensive care units (NICUs), newborns with perinatal hypoxic ischemic encephalopathy (HIE) undergo continuous monitoring of various vital parameters. In these patients, monitoring the background activity of electroencephalogram (EEG) is an optimal method to estimate the degree of HIE severity and to assess subsequent improvement (or deterioration) of brain function. EEG is thus a valuable diagnostic and prognostic tool in NICUs (Monod et al., 1972; Watanabe et al., 1980; Pezzani et al. 1986; Murray et al., 2009). Due to the complex morphology of the EEG, a high level of expertise is required to interpret this signal. However, around the clock support of clinical neurophysiologists is usually not readily available in NICUs. On the other hand, many treatment decisions based on EEG findings need to be prompt, such as administration of therapeutic hypothermia for moderate to severe neonatal HIE or treatment of seizures. This means that there is a gap between the existing large need for EEG monitoring and its limited availability in NICUs.

Even though automated EEG analysis has been used as a research tool for several decades, visual interpretation of EEG remains the 'gold' standard, despite the rather high inter-rater disagreement (Walsh et al., 2011). For instance, automated EEG segmentation algorithms have been previously developed (e.g. Barlow et al., 1981; Krajca et al., 1991). More specifically, in term and premature newborns, research has been focused on analysis of certain EEG patterns. For example, effective sleep wake cycle detection methods (Scher et al., 2004; Gerla et al., 2009), approaches for EEG background state detections (Lofhede et al. 2010) and automated neonatal seizure detectors (Gotman et al., 1997; Deburchgraeve et al., 2008; Temko et al., 2011; Cherian et al., 2011) have been proposed.

The current major bottlenecks for the development of reliable automated EEG analysis methods seem to be the complex morphology of the EEG signal, inter-rater disagreement, the small size of used datasets and the presence of artifacts. Significant progress has been achieved with EEG artifact-removal tools. For example, methods for removing muscle, electrocardiogram, pulsation and respiration artifacts have been published (e.g. Joyce et al., 2004; Klemm et al., 2009; De Vos et al., 2010, De Vos et al., 2011). However, these methods are mostly tuned for one or few specific artifacts, whereas in fully automated analysis of EEG background, a diverse range of artifacts are encountered that adversely affect system's performance. For example, electrode and wire problems, movement and transient muscle artifacts, to name a few, will hinder the detection accuracy. Therefore, despite many efforts, there is an unmet need for a robust and reliable automated real-time EEG analysis system for use in NICUs.

We have developed an automated method (*neoGuard_A*, hereafter called only algorithm A) for the detection of *dynamic* interburst intervals (*dIBIs*) in order to classify EEG discontinuities in neonatal EEG (Matic et al., 2013a, companion paper). The newly introduced parameter *dIBI* represents an extension of the classical interburst interval (IBI) and incorporates various amplitude levels of EEG discontinuity into its definition. The algorithm A, as shown in our preliminary studies (Matic et al., 2012; Matic et al., 2013a, companion paper), detects *dIBI* patterns with a high sensitivity. However, due to the presence of artifacts and ambiguous EEG patterns, algorithm A produces a significant number of *misclassified dIBIs* as well. Numerous hindering factors affect its performance, thereby resulting in *uncertain* or false detections. We describe here further refinements of algorithm A that improves the reliability of *dIBI* detections.

The main objective of automated background EEG analysis in neonates with HIE is not to detect every individual *dIBI*, but rather to detect a subset of *definite dIBIs* while imposing extremely high detection accuracy. Subsequently, analyzing duration and amplitude of *definite dIBIs* within this subset, we can accurately assess the severity of discontinuity of

the background EEG under investigation. In this paper, we propose a method (*NeoGuard_B*, hereafter called only algorithm B) to distinguish *definite dIBI* detections from *misclassified* ones. Previously, we classified *dIBIs* into four duration groups and showed that *dIBI* amplitude values are significantly different between them (Matic et al., 2013a, companion paper). The detected *dIBIs* can be categorized as *definite* if the estimated amplitude of the suppressed period is within an acceptable range for a given duration. Moreover, among the four defined *dIBI* duration groups, the overall morphology of *dIBI* patterns is significantly different and we need to consider this when performing the refinement step. With these considerations, further refinement analysis will be performed independently by assigning a specific classifier to each corresponding *dIBI* duration group. To distinguish *definite dIBIs*, we optimize four Least Squares Support Vector Machines classifiers (LS-SVM) (Suykens et al., 1999) to work in parallel. Classifiers input feature vectors are reliability parameters developed to characterize and describe *dIBI* detection certainty.

Finally, in order to validate the performance of the overall system (A+B) visual and automated *dIBI* detections are compared. An expert EEG reader examined individual *dIBIs*, detected in eight 30min cEEG segments selected randomly from an unseen dataset of eight neonates with HIE. After the refinement of *dIBI* detections using algorithm B, significantly improved good detection rate is achieved. Furthermore, we show how median *dIBI* duration and amplitude values can reliably predict the background EEG grade. This correlation is demonstrated on extensive, non-preselected 2h cEEG epochs that were visually scored by an experienced clinical neurophysiologist. Thus, we demonstrate that our system achieves a high level of reliability to classify background EEG discontinuity and to monitor its evolution.

2. Methods

2.1. Dataset

Data for this study has been recorded at the Sophia Children's Hospital, Erasmus University Medical Center, Rotterdam, the Netherlands. The database consists of 46 (=38+8) full-term neonates with perinatal asphyxia who underwent continuous EEG (cEEG) monitoring. The sampling frequency was 256 Hz. The recordings were started 6-48 hours post partum (PP), using a full set of 17 EEG electrodes (Fp1,2, F3,4, C3,4, Cz, P3,4, F7,8, T3,4, T5,6, O1,2), whereas in some patients a reduced set with 13 electrodes was used (P3,4 and F3,4 were not used). EEG signals were analyzed using bipolar montage and number of channels was 20 (or 12). In addition, the EEG registrations were anonymized and converted to European Data Format.

The preprocessing step in this work is the same as described in (Matic et al., 2013a, companion paper). We used the same dataset DB as described in (Matic et al., 2013a) to optimize the LS-SVM classifiers. For validation, we used two new datasets: dataset DB4 and dataset DC.

Dataset DB4 consists of the same 38 neonates as dataset DB (see also supplemental data in Matic et al., 2013a). However, we selected 2h non-overlapping cEEG segments, ensuring that they are recorded at least 4h after the segments that we used for dataset DB. From each patient we selected equidistantly four epochs of 2h across EEG recording. For example, irrespective of the post partum time when the recording started, for dataset DB we chose the cEEG segment from 1-2h, whereas for dataset DB4 we use the following time intervals 6-8h, 12-14h, 18-20h and 24-26h.

Dataset DC consists of eight new neonates with predominantly mild and moderate EEG background abnormality. This selection was done as we feel that a true test of the

algorithm would be to accurately classify such patients (with predominantly 5s<*dIBI*<15s). From each neonate, 30 minutes of EEG was randomly selected. More specifically, we used 6 epochs of 5-min duration each, distributed equidistantly across 2 hours of EEG recording.
Neonates in datasets DA and DB (described in Matic et al., 2013a), and in dataset DC were all mutually exclusive. Thus, the total number of full-term neonates with postasphyxial encephalopathy that we analyzed in both companion papers was 53 (=7+38+8).

*2.2. **NeoGuard_B**: reliable refinement of the detected dIBIs*

The complete algorithm for *dIBI* detection consists of two parts: *NeoGuard_A* (Matic et al., 2013a, companion paper) for automated *dIBI* detection and *NeoGuard_B*, for the refinement of detected *dIBIs*. A flow chart of the algorithm is depicted in Fig. 1. First, a large set of *dIBI* candidates is detected using *NeoGuard_A*. Next, the reliability parameters (features vectors) are calculated for each detected *dIBI*. They are designed to describe the confidence level of *dIBIs* detection accuracy. Depending on the *dIBI* duration, we split *dIBIs* into four duration groups. Accordingly, four different LS-SVM classifiers would be applied to assess whether the detected *dIBIs* are *definite* or whether they should be excluded from further analysis. For further assessment of background EEG abnormalities, only *definite dIBIs* would be used.

Fig. 1 here

2.3. Necessity for the refinement of the *dIBI* detections

Main reason to refine *dIBI* detections is to examine whether the amplitude of the suppressed period is in the adequate range. During visual analysis, a clinical neurophysiologist ascertained the amplitude and frequency (maximum upper bounds) of EEG activity within the suppressed periods. In case that estimated amplitude is excessively high, *dIBI* detection would be considered as interrupted. In addition, the reliability of the background EEG analysis system is adversely affected by two major factors: the presence of artifacts and the difficulty to visually interpret the duration of EEG discontinuity (*dIBI*) due to complexity of the EEG signal itself. Therefore, certainty of *dIBI* detections is related to the variability of the EEG signal. In some cases, when the variability of EEG patterns is too high (*ambiguous* EEG discontinuity), it would be difficult to visually interpret the exact duration of the discontinuity. Then, it is necessary for an automated system to efficiently discriminate the *ambiguous* EEG patterns from *definite dIBIs*. This uncertainty in *dIBI* classification is not a limitation of the presented algorithm A, but a challenge inherently present in automated analysis of mild and moderate EEG discontinuities.

In Fig. 2, we illustrate this difficulty. It shows the challenge to assess amplitude and duration of EEG discontinuities in a term neonate with moderate HIE. The *ambiguous* EEG pattern would lead to high disagreement between human raters who would visually mark the duration of the *dIBIs*. However, an automated algorithm similar to the one presented in literature (Lofhede et al., 2010), would process the whole segment and would make the classification into burst and suppression periods only. Suppressed EEG activity from the 9^{th} till the 17^{th} second would be classified accurately, whereas *ambiguous* EEG discontinuity, lasting from the 20^{th} till the 50^{th} second, would be variedly classified. In our approach, as visual classification of the latter segment is difficult, we would tend to exclude these detections as *misclassified dIBIs*.

Fig. 2 here

Therefore, out of all detected *dIBI* candidates, we would keep only *definite dIBIs* in the refinement step and further perform accurate background EEG analysis. The excluded detections, named *misclassified dIBIs* (MC), can be categorized into two subsets. First, a false positive detection is classified as *type I,* if the detected *dIBI* duration does not correspond to the actual, visually interpreted duration. More specifically, detected *dIBI* can be falsely shortened or falsely prolonged due to one of the following reasons:

- MC1: artifacts or true paroxysmal activity, such as seizures, falsely interrupt suppression of *dIBI*, resulting in falsely shortened *dIBIs*. The most frequent causes are transient artifacts present on many EEG channels that are not accurately removed (e.g. electro-oculogram or movement artifacts).
- MC2: situations when bursts are expressed on the majority of the EEG channels with an amplitude strictly <10μV causing falsely prolonged *dIBI* detections as the low amplitude bursts were missed. This was encountered during the early phases of cEEG recordings (<24h post partum).
- MC3: missed bursts in situations when they were present on less than 50% of the bipolar EEG channels. In visual studies, researchers discard such suppressed periods as interrupted and do not include them in final analysis (Biagioni et al., 1999; Menache et al., 2002). Nevertheless, we include this group in erroneous detections.
- MC4: An EEG pattern detected by algorithm A does not fit into our *dIBI* definition (described in Matic et al., 2013a, companion paper). For example, patterns similar to the EEG activity from the 20^{th} till the 50^{th} second in Fig 2. can be variedly detected. However, within this EEG interval, excessive amplitude variability is present and clear transitions with bursts (or more continuous EEG segments) are lacking.

False positive detections, *type I,* are excluded in the refinement step as they produce misclassification in our ultimate goal of automated EEG-based assessment of HIE severity. On the other hand, we defined a subset of false positive *dIBI* detections, *type II*, in case that *dIBI* duration detected by the algorithm A is the same as interpreted by visual EEG rater. This group of false positives would not lead to misclassification of background EEG grades. However, we decided to exclude those *dIBIs* due to the following reasons:

- MC5: presence of many artifacts and/or epileptic seizures within *dIBI* on many EEG channels. Despite the presence of this activity, the algorithm correctly classifies the duration of the *dIBI*. However we exclude these detections from analysis as further *dIBI* amplitude assessment can be significantly biased.
- MC6: morphology of *dIBI* complex does not fit into our *dIBI* definition. For example, in Fig. 3, algorithm A detected *dIBI* lasting from the 10^{th} till the 21^{st} second. Though the detected EEG interval appears to be suppressed, it does not represent *definite dIBI*. In this particular case, the EEG patterns before and after the suppression cannot be confidently regarded as bursts. In addition, some amount of paroxysmal EEG activity within the suppressed period interrupts the *dIBI*.

Fig. 3 here

B1. Framework for reliability parameterization of *dIBI*

To distinguish *dIBI* detections based on the degree of certainty, we parameterize the 'burst-suppression-burst' complex. Each parameter corresponds to the guiding rule used by

clinicians during meticulous visual interpretation of EEG discontinuities. Some of the parameters are optimized to confirm *definite dIBIs*, whereas others are tuned to exclude *misclassified dIBI* detections.

1) *Suppression* is defined as a median single value of the rectified EEG signal within the suppressed *dIBI* period across all EEG channels.
2) *Flatness* is calculated for each EEG channel independently within the suppressed *dIBI* period. We adjusted two horizontal border lines, so that they enclose 95% of all EEG samples within the *dIBI*. The minimum possible distance between these two horizontal lines represents the parameter *flatness* (Fig.4 and Matic et al., 2013a, companion paper, Fig. 5). Next, the *flatness* is calculated for each EEG channel and the obtained values are sorted into an ascending order. Subsequently, these values are split into four equal groups. For each group, a median value is calculated, thus obtaining four parameters that estimate the suppression level of the *dIBI*.
3) *Longest*: within the *dIBI*, for each EEG channel, we calculate the longest interval of the low amplitude segment classes that are not interrupted by a medium or high amplitude activity (as defined in Matic et al., 2013a, companion paper). If several consecutive low amplitude segments are present next to each other we will merge them into a single one. This parameter ranges from 0% (no low amplitude segments) to 100% (only low amplitude segments). It is an important descriptor for decisions whether the suppressed period is interrupted, especially in cases when higher amplitude EEG activity is distributed randomly across suppressed period. In the same way, as with the parameter *flatness*, we sort all values calculated for each channel in an ascending order and calculate 4 parameters as median value of the corresponding quartile groups.
4) *Number of channels*: For the presumed duration of the *dIBI* (suppressed part), we calculate the mean value of the Low amplitude Temporal Profile (LTP) signal. Next, this value (number of EEG channels expressing LTP signal) is divided with the total number of (bipolar montage) EEG channels. As *dIBI* was thresholded at a value of one more than half the number of total EEG channels, this parameter will be in the range from 55% to 100%.
5) *Transitioning*: This parameter examines the presence of bursts and how distinguishable burst/suppression segments are. Six seconds of the EEG signal are selected with a center exactly at the burst/suppression transition point as detected by algorithm A (Fig 4., two upper plots). Next, this signal is decomposed using Discrete Wavelet Transform (DWT) (Mallat et al., 2008). We applied Daubechies 4 mother wavelet and 4 levels of decompositions. In this way, the burst part (3s) is characterized with wavelet coefficients that express higher absolute values, whereas the suppressed part (3s) is characterized with wavelet coefficients close to zero (Fig. 4, two lower plots). To further enhance the differences between burst and suppression segments, we sort absolute values of wavelet coefficients into an ascending order. Then, iteratively, starting from the smallest values, we set small wavelet coefficient values to zero. We repeat this process while keeping more than 90% of the original signal power within the remaining wavelet coefficients. In this way, the sparsely approximated signal preserves the abrupt increase in activity of the burst period, whereas the majority of wavelet coefficients within the suppressed period are set to zero. The percentage of power retained by wavelet coefficients within the burst part compared to the total power of all wavelet coefficients, after the sparse approximation, determines the *transitioning* parameter. Furthermore, this parameter is averaged across all EEG channels. Thus, if the burst/suppression transition represents a clear cut-off, the value

of *transitioning* parameter is expected to be approximately 90-100%. However, if this value is around 50-65% it is doubtful whether a distinguishable burst/suppression alternation exists. Furthermore, as both transitions, at the beginning and at the end of the *dIBI*, are important, for every *dIBI* we calculate 2 *transitioning* parameters. In Fig 4, examples of mild (shorter *dIBI*) and severe (longer *dIBI*) EEG discontinuities are depicted.

Fig. 4 here

6) *NLEO local maxima*: In some cases, bursts can occur synchronously with relatively low amplitude (<10 μV) and can be missed by the algorithm A – MC2. Another scenario is that a burst is present on less than 50% of EEG channels – MC3. This can produce a false merging of two shorter *dIBIs* into a longer one. To examine the presence of missed bursts, we apply a Nonlinear Energy Operator (NLEO) as a very effective method for detection of bursts and dynamic EEG activity (Palmu et al., 2010). NLEO is calculated using the following formula:

$$\psi(x[n]) = x^2[n] - x[n-1] \cdot x[n+1]$$

We calculate an average NLEO across all EEG channels and use maximal value of this signal as a parameter.

B2. Creating a reliable subset of detected *dIBIs*

Parameters described in (B1) are used as input feature vectors into Least Squares Support Vector Machine (LS-SVM) classifiers (Suykens et al., 1999). The objective of the classifier is to estimate whether the newly detected *dIBI* is *definite* - {1} or *misclassified* - {0}. Values obtained by visual checking {0, 1} are concatenated with the *dIBI* feature vectors. Since *dIBIs* are split into four groups depending on their duration (Table 1), four LS-SVM classifiers are optimized independently.

To optimize classifiers, four mutually exclusive training datasets were created. For each dataset, 80% of *dIBIs* were randomly selected from each *dIBI* duration group. The remaining 20% of *dIBIs* from each group were used to test the corresponding LS-SVM classifiers. The LS-SVMlab v1.8 toolbox implementation was used in this study (www.esat.kuleuven.be/sista/lssvmlab, De Brabanter et al., 2011). In all cases, a Gaussian kernel was applied. Tuning of the parameters was conducted in two steps. First, coupled simulated annealing is performed (Xavier De Souza et al., 2010) and afterwards, a second optimization procedure (simplex) was applied to perform a fine-tuning step. The five-fold cross-validation misclassification error was used as an optimization criterion.

3. Results

3.1. Performance of the reliability LS-SVM classifiers

Processing dataset DB using algorithm A yielded 4408 detected *dIBI* candidates (Table 1). These *dIBIs* were visually checked in terms of detection certainty. During this step, 2273 *dIBIs* were accepted as correctly detected, whereas 2135 were excluded (analysis in Matic et al., 2013a, companion paper).

Table 1 here

Performance of the 4 classifiers is illustrated using Receiver Operating Characteristic (ROC) curves presented in Fig. 5 (A to D). High Area Under the Curve (AUC) values are achieved for all 4 classifiers. Longer *dIBIs* tend to have more definite morphology, therefore, the corresponding classifiers showed slightly better performance.

Fig. 5 (A, B, C, D) here

In addition, the test dataset is used to validate the performance of the LS-SVM classifiers (Fig. 6). The lengths of the bars (A) are adjusted to fit the corresponding percentage values as the number of *dIBIs* differed among groups. For every *dIBI* group, the first bar (A) represents the distribution of *definite dIBIs* (blue - $A_{\{1\}}$) and *misclassified* (red - $A_{\{0\}}$) as marked visually by an experienced clinical neurophysiologist (PJC). After the refinement step, the reliability classifier selects a subset of *dIBIs.* Consequently, the size of the second bar ($B_{\{1\}}$) is represented by proportionally shrinking the size of the bar (A). Here, *dIBIs* that are retained in the reliable subset ($B_{\{1\}}$) and previously marked as *definite* ($A_{\{1\}}$) are shown in blue ($B_{\{1\}} \cap A_{\{1\}}$). The red bar segments corresponds to *misclassified* detections ($B_{\{1\}} \cap A_{\{0\}}$). Comparing the ratio of *definite* and *misclassified dIBIs* before and after the refinement step, a substantial increase in accuracy is achieved for each *dIBI* group.

Fig. 6 here

3.2. Visual validation of *dIBI* detections

In order to illustrate how powerful the complete algorithm can be, we present the validation results on an independent dataset DC. This dataset consisted of eight new neonates and 30min of EEG was analyzed per neonate. First, the EEG data were processed only with the algorithm A and *dIBI* candidates were detected. Next, an experienced clinical pediatric neurologist (KJ) scored the detected *dIBIs* as *definite* or not. In this experiment, the human rater also used polygraphy channels to distinguish artifacts from true EEG activity.

In total, 835 *dIBIs* were detected by algorithm A. We compare the results before and after the refinement step using the reliability classifiers in Table 2. Comparing the values in the second and third columns, we can see that a substantial number of *dIBIs* automatically detected by algorithm A were marked as *misclassified* by the expert EEG reader. Thus, there is a necessity for the refinement step. In the fourth column, we can see that the LS-SVM classifiers retain most of the visually marked definite *dIBIs.* In clinical practice, to reliably estimate the background EEG abnormality, it is important that a sufficient number of *dIBIs* is retained (e.g. at least 20 within 1h of cEEG recording). Third, within the retained sets of *dIBIs*, there is a significant improvement after the refinement step in the number of correctly detected *dIBIs* as compared to detections using only algorithm A. Good detection rate has been increased in all four groups, respectively from 68%, 77%, 75% and 57% to 98%, 97%, 88% and 95%. That is, significant majority of *dIBIs* detected by the complete detection system belong to the group that has been previously marked as *definite* by the human EEG rater. Thus, though the second expert EEG reader (KJ) had not been involved in the development phases of the algorithm A, high agreement with the algorithm has been achieved. Finally, the number of false positive *dIBIs* is negligible for each duration group, ranging from 2% to 12% (Table 2, column 5).

Table 2 here

3.3. Duration and amplitude of *dIBIs* vs. visual background EEG scoring

The main objective of our automated system is to apply it as a decision-support system to assess the severity of EEG background discontinuity. Thus, another way to validate the significance and usefulness of our method is to show how it can be applied for automated scoring of background EEG abnormalities. In this part, we show the results of fully automated processing of cEEG epochs within dataset DB4. It consisted of 38 neonates and 2h cEEG epochs were analyzed. From each neonate, we equidistantly selected four 2h cEEG segments across EEG recording. An experienced clinical neurophysiologist (PJC) visually assessed background EEG of these neonates.

Background EEG abnormalities were classified into mild, moderate and severe classes. The applied grading system was adapted from the one proposed in (Murray et al., 2009) resulting in: a) mild - approximately *dIBIs*<5s; poorly organized sleep wake cycle b) moderate – approximately 5s ≤ *dIBI* < 10s c) severe abnormality *dIBIs* > 10-20s, characterized by prolonged and marked suppressions. Some neonates are not described with only one class due to evolution of the background EEG activity. For instance, the background EEG abnormalities of a neonate with recovering HIE may be graded as: severe (21-23h PP), severe (27-29h PP), moderate (33-35h PP) and mild (39-41h PP).

At this stage, during the development phase of the algorithm, we have restricted ourselves to duration and amplitude of the EEG discontinuities and do not aim to perform comprehensive automatic grading of the background EEG activity. (For the latter, many other parameters need to be taken into account such as content and morphology of EEG bursts, sleep-wake cycles, EEG asymmetry, asynchrony and presence of sharp waves etc.). Within each 2h EEG segment, median duration and median amplitude of *dIBIs* were calculated to characterize the trend of the EEG background activity. For the amplitude assessment, parameter *flatness3* was applied (Matic et al., 2013a, companion paper). After processing the dataset DB4 in this way using algorithms A and B, we obtained 152 detected *dIBIs* for each cEEG segment. This is shown in Fig. 7 where each data point corresponds to a 2h cEEG segment (4 data points per neonate, representing the entire length of cEEG monitoring). Visually scored background EEG abnormalities are depicted as: mild (blue), moderate (red) and severe (black). Next, we applied two quadratic classifiers to determine the boundaries between the classes: mild vs. moderate and moderate vs. severe. In Fig. 7, a very efficient separation of the classes is achieved. The borders between classes are depicted with two ellipsoids (magenta). The larger one separates mild and moderate class, whereas the smaller one distinguishes moderate and severe class. Moreover, introducing amplitude of *dIBIs* as a feature, we enhanced the *separation* between the classes compared to use of only duration of *dIBIs*. Especially, this can be observed in the separation between mild and moderate classes. Therefore, incorporating amplitude into *dIBI* definition and its monitoring enabled us to better classify background EEG discontinuities as graded by an experienced clinical neurophysiologist.

Fig. 7 here

4. Discussion

We present an algorithm for automated *dynamic* interburst interval detection in EEGs of full-term neonates with postasphyxial encephalopathy ranging from mild to severe. The algorithm consists of two parts and the first one (A) detects *dIBI* candidates with high

sensitivity. The second part (B) calculates reliability parameters for each detected *dIBI* and refines the detection accuracy. In this work, our objective was to identify a large set of correctly detected *dIBIs* that would be visually marked by an experienced EEG interpreter and confirmed with high inter-rater agreement. As part of this strategy, *uncertain* and *ambiguous* EEG patterns would be excluded, reducing significantly the number of *misclassified* detections. To perform these steps, four LS-SVM classifiers are designed to replicate guiding rules and decisions brought by human EEG reader experts. Furthermore, conducted experiments confirmed that the proposed system efficiently analyzes non-preselected cEEG epochs and tackles the presence of artifacts and seizures. In this way, effects of many hindering factors that adversely affect automated analysis of EEG signal are significantly reduced.

In the companion paper to this article, we demonstrated a statistically significant relation between duration and amplitude of EEG discontinuity (Matic et al., 2013a). Furthermore, other reliability parameters were compared between *dIBI* groups of different durations. For all of these features, a significant difference was found as overall *dIBI* morphology depends on its duration. Milder EEG discontinuities (<10s) were more difficult to detect and to accurately characterize compared to longer EEG discontinuities. They expressed higher amplitude of the suppressed period and smoother transitions with burst segments. With these findings, four reliability LS-SVM classifiers are designed to work in parallel, thereby improving the refinement step of algorithm B.

We identified two groups of *misclassified dIBIs, type I* and *type II*, with respect to how the detected duration would affect further grading of HIE severity. Misclassification errors, *type I*, that produce bias in the further assessment of background EEG grade are especially tackled during the development of reliability parameters that assign confidence levels to detected *dIBI* complexes. We showed that the number of *misclassified dIBIs* is significantly reduced by using reliability classifiers. Moreover, the remaining *misclassified dIBIs*, after the refinement step, would mostly fit into *misclassified* group *type II*, that would not significantly bias the assessment of background EEG abnormalities. This group consists of EEG discontinuities with morphology very similar to *definite dIBIs*. In fact, the already achieved high detection accuracy can be regarded as even more reliable. This was confirmed when we found a significantly increased agreement between the human rater and the algorithm during the visual validation of individual *dIBI* detections. Nevertheless, in future studies, we would like to analyze *misclassified dIBIs* in more detail and to further refine our exclusion criteria.

Few research groups have tried to tackle the problem of suppression/burst detections in full-term asphyxiated neonates and/or to develop methods for automated grading of background EEG abnormalities. A significant contribution has been presented within the work of (Lofhede et al., 2008; Lofhede et al. 2010; Flisberg et al., 2011). However, the development of this method included only a small number of neonates (six), who predominantly expressed severe and prolonged background EEG discontinuities (Lofhede et al., 2008).

In (Korotchikova et al., 2011), authors demonstrated that a combination of quantitative EEG (qEEG) features can be applied to predict background EEG abnormality as determined by experienced clinical neurophysiologists on one hour segments of EEG. It was designed to replicate experts' grading of HIE severity, resulting in a single output value. Typically, this value would represent a grade from 1 to 4, which helps to partly replace visual classification of EEG. However, this output, which uses a combination of many qEEG features, does not reveal new insights into the various characteristics of EEG discontinuity in neonatal HIE and does not help to refine prognostication. It is also difficult to estimate how the proposed system would tackle many hindering factors like artifacts and seizures that would inevitably bias the values of qEEG parameters. Compared to this study, our dataset included major artifacts and

electrographic seizures and represented non-preselected real case scenarios. Despite this, we could detect and predict background EEG abnormalities with high discrimination accuracy. We feel that monitoring EEG discontinuity in its various forms (*dIBI*) is a more refined approach as we can more accurately analyze speed of HIE recovery. According to Murray et al., this parameter may prove to have significant prognostic value in HIE recovery (Murray et al., 2009).

Other quantitative approaches have analyzed 'burst/suppression' patterns in premature EEG (Palmu et al., 2010; Jennekens et al., 2011; Mitchell et al., 2013). Compared to these, the *dIBI* parameter includes more complex burst-suppression-burst patterns, encompassing much broader range of EEG discontinuities.

Due to brain recovery and background EEG evolution in mild and moderate HIE, EEG discontinuity patterns significantly change in morphology. At the beginning of the recordings, burst patterns tend to be low in amplitude, with extremely attenuated suppressed segments. In case of recovery of hypoxic brain injury, EEG activity during both suppressed and burst periods will become more pronounced and overall EEG amplitude will increase, whereas duration of *dIBIs* will decrease. This will result in an overlap between classes at various time points that the pre-defined qEEG parameters will not be able to distinguish. Thus, encountered scenarios may include bursts registered at 12h post partum that are lower in amplitude than suppression segments at 48h post partum. Quantified EEG parameters used for supervised learning (Lofhede et al., 2010) will most likely fail to detect such changes in EEG morphology. Our method detects suppressions with high sensitivity and the presence of bordering bursts is examined afterwards. Next, reliability parameter, *transitioning*, compares how burst/suppression patterns are relatively distinguishable regardless of their amplitude values. Furthermore, as *dIBIs* become shorter with more active suppressions, corresponding duration related LS-SVM classifier would be applied to classify them as *definite dIBIs*. Approaches presented in (Lofhede et al., 2010; Palmu et al., 2010; Jennekens et al., 2011) are not sensitive to the evolution of background EEG activity. On the other hand, our method is adaptable to dynamic changes in the background EEG, which is a distinct advantage.

Finally, even though our definition of *dIBI* incorporates amplitude and duration parameters and takes into account the various types of transitioning between bursts and *dIBIs*, it could be argued that an attempt to represent a complex and chaotic signal like EEG with a single parameter is fundamentally flawed. However, in encephalopathic neonates, we would expect a relative simplification of EEG patterns, resulting in discontinuity of the EEG and the appearance of (at least a few) definite *dIBIs* which would be detected by our automated system. Since our aim with automated *dIBI* detection is to develop a method to grade HIE and follow its evolution in neonatal encephalopathy and not to encapsulate the entire range of complexities of the EEG signal from normal to abnormal, we feel that our approach is justified. Furthermore, the advantage of our refinement step is that it selects only highly certain *dIBI* detections, which would have very good inter-rater agreement. To further investigate the potential of the *dIBI* parameter for scoring background EEG abnormalities and its prognostic value, it is necessary to perform multi-center validation studies with larger datasets. This analysis would also aim towards the development of a widely acceptable EEG background grading system in HIE using data-driven rules and eventually use it to guide treatment decisions.

Acknowledgments

We thank the neurotechnologists who made the high quality EEG recordings and patients and parents for their co-operation.

References

Barlow JS, Creutzfeldt OD, Michael D, Houchin J, Epelbaum H. Automatic adaptive segmentation of clinical EEGs. Electroencephalogr Clin Neurophysiol 1981;51: 512–25.

Biagioni E, Bartalena L, Boldrini A, Pieri R, Cioni G. Constantly discontinuous EEG patterns in full-term neonates with hypoxic-ischaemic encephalopathy. Clin Neurophysiol 1999;110:1510–5.

Cherian PJ, Deburchgraeve W, Swarte RM, De Vos M, Govaert P, Van Huffel S, et al. Validation of a new automated neonatal seizure detection system: a clinician's perspective. Clin Neurophysiol 2011;122:1490–99.

De Brabanter K, Karsmakers P, Ojeda F, Alzate C, De Brabanter J, Pelckmans K, et al. LS-SVMlab Toolbox User's Guide version 1.7. Technical Report; ESAT-SISTA, K.U. Leuven; 2011.

Deburchgraeve W, Cherian PJ, De Vos M, Swarte RM, Blok JH, Visser GH, et al. Automated neonatal seizure detection mimicking a human observer reading EEG. Clin Neurophysiol 2008;119:2447-54.

De Vos M, Ries S, Vanderperren K, Vanrumste B, Alario F-X, Van Huffel S, et al. Removal of muscle artifacts from EEG recordings of spoken language production. Neuroinformatics 2010;8:135-50.

De Vos M, Deburchgraeve W, Cherian PJ, Matic V, Swarte RM, Visser GH, et al. Automated artifact removal as preprocessing refines neonatal seizure detection. Clin Neurophysiol 2011;122:2345-54.

Flisberg A, Kjellmer I, Löfhede J, Lindecrantz K, Thordstein M. Prognostic capacity of automated quantification of suppression time in the EEG of post-asphyctic full-term neonates. Acta Paediatr 2011;100:1338-43.

Gerla V, Paul K, Lhotska L, Krajca V. Multivariate analysis of full-term neonatal polysomnographic data. IEEE Trans Inform Technol Biomed 2009; 3:104–10.

Gotman J, Flanagan D, Zhang J, Rosenblatt B. Automatic seizure detection in the newborn: methods and initial evaluation. Electroencephalogr Clin Neurophysiol 1997;103: 356-62.

Joyce CA, Gorodnitsky IF, Kutas M. Automatic removal of eye movement and blink artifacts from EEG data using blind component separation. Psychophysiology 2004;41:313–25.

Klemm M, Haueisen J, Ivanova G. Independent component analysis: comparison of algorithms for the investigation of surface electrical brain activity. Med Biol Eng Computing 2009;47:413–23.

Krajca V, Petránek S, Patáková I, Värri A. Automatic identification of significant graphoelements in multichannel EEG recordings by adaptive segmentation and fuzzy clustering. Int J Biomed Comput 1991;28:71–89.

Löfhede J, Thordstein M, Löfgren N, Flisberg A, Rosa-Zurera M, Kjellmer I. Automatic classification of background EEG activity in healthy and sick neonates. J Neural Eng 2010;7:16007. doi: 10.1088/1741-2560/7/1/016007.

Löfhede J, Löfgren N, Thordstein M, Flisberg A, Kjellmer I, Lindecrantz K. Classification of burst and suppression in the neonatal electroencephalogram. J Neural Eng 2008;5:402-10.

Mallat S. A Wavelet Tour of Signal Processing: The Sparse Way, 3rd ed. Academic Press, 2008.

Matic V, Cherian PJ, Jansen K, Koolen N, Naulaers G, Swarte RM, et al. Automated EEG inter-burst interval detection in neonates with mild to moderate postasphyxial encephalopathy. Conf Proc IEEE Eng Med Biol Soc. 2012; 2012:17-20. doi: 10.1109/EMBC.2012.6345860.

Monod N, Pajot N, Guidasci S. The neonatal EEG: statistical studies and prognostic value in full-term and pre-term babies. Elecroencephalogr Clin Neurophysiol 1972;32:529–44.

Murray DM, Boylan GB, Ryan CA, Connolly S. Early EEG findings in hypoxic-ischemic encephalopathy predict outcomes at 2 years. Pediatrics 2009;124:e459–67.

Palmu K, Wikstrom S, Hippelainen E, Boylan G, Hellstrom-Westas L, Vanhatalo S. Detection of 'EEG bursts' in the early preterm EEG: visual vs. automated detection. Clin Neurophysiol 2010;121:1015-22.

Pezzani C, Radvanyi-Bouvet MF, Relier JP, Monod N. Neonatal electroencephalography during the first twenty-four hours of life in full-term newborn infants. Neuropediatrics 1986;17:11–8.

Scher MS. Automated EEG-sleep analyses and neonatal neurointensive care. Sleep Med 2004;5:533–40.

Temko A, Thomas E, Marnane W, Lightbody G, Boylan G. EEG-based neonatal seizure detection with Support Vector Machines. Clin Neurophysiol 2011;122:464–73.

Xavier de Souza S, Suykens J, Vandewalle J, Bolle D. Coupled simulated annealing. IEEE T Syst Man Cyb 2010;40:320–35.

Walsh BH, Murray DM, Boylan GB. The use of conventional EEG for the assessment of hypoxic ischaemic encephalopathy in the newborn: A review. Clin Neurophysiol 2011;122:1284-94.

Watanabe K, Miyazaki S, Hara K, Hakamada S. Behavioral state cycles, background EEGs and prognosis of newborns with perinatal hypoxia. Electroencephalogr Clin Neurophysiol 1980;49:618–25.

Legends to figures

Figure 1. Flow chart of the algorithm for automated detection of *dynamic IBIs*. *NeoGuard_A* consists of 3 stages and it detects *dIBIs* with high sensitivity (Matic et al., 2013a, companion paper). In *NeoGuard_B, dIBIs* are parameterized (B1) and corresponding classifiers estimate the reliability of detected *dIBIs* (B2).

Figure 2. Moderately abnormal EEG in a term neonate with moderate HIE. A clear EEG discontinuity is observed from the 9^{th} till the 17^{th} second, followed by EEG activity that is difficult to accurately classify (containing *ambiguous* discontinuities) lasting from the 20^{th} till the 50^{th} second. Black rectangles correspond to automated *dIBI* candidates detected using algorithm A.

Figure 3. Severe background EEG in HIE neonate. Detected *dIBI* with algorithm A, lasting from the 10^{th} till the 21^{st} second, was excluded during visual classification. Although, this interval indeed fulfilled the *dIBI* definition criterion as being attenuated and suppressed, the bursts (transitioning points) cannot be regarded as confident. This *dIBI* candidate would be also excluded in the refinement step due to effect of the *transitioning* parameter that examines transitions between burst/suppression segments. In this case, clear-cut transitions are missing (values lower than 65%).

Figure 4. *Transitioning* and *flatness* parameters are illustrated for mild and severe EEG discontinuity. The first 3s of the signal represent a burst period, whereas the last 3s correspond to the suppressed segment. In two lower figures, wavelet coefficients are depicted in black for zero values and in white and yellow for larger absolute coefficient values. After sparse approximation, large wavelet coefficients would be retained mainly within the abrupt burst activity. Therefore, the calculation of *transitioning* parameter efficiently characterizes the presence of distinguishable burst/suppression alternations. These two examples also illustrate the differences in *dIBI* morphology among *dIBI* duration groups. In addition, the *flatness* parameter is depicted and represents the distance between the two horizontal grey lines that enclose the suppressed part of the signal.

Figure 5. Receiver Operating Characteristic (ROC) curves presenting the performance of reliability classifiers for 4 different *dIBI* duration groups: A-group I ($3s \leq dIBI < 5s$), B-group II ($5s \leq dIBI < 10s$), C-group III ($10s \leq dIBI < 20s$) and D-group IV ($20s \leq dIBI$). Longer *dIBIs* (group III and IV) showed better performance due to more definite morphology associated with longer *dIBIs*.

Figure 6. (A) *definite* and *misclassified dIBIs* are depicted for each *dIBI* duration group. Blue bar segments represent *dIBIs* visually marked by human rater as *definite* - $A_{\{1\}}$, whereas the red ones represent excluded *dIBIs* - $A_{\{0\}}$. The improvement after the refinement step using LS-SVM classifiers is shown by ($B_{\{1\}}$). For every *dIBI* group, within the reliable subset $B_{\{1\}}$, ratio of *definite* (blue) and *misclassified dIBIs* (red) are presented.

Figure 7. Median duration and amplitude of *dIBIs* are plotted as a single data point for each 2h cEEG epoch (4 data points per neonate). Background EEG abnormality of the corresponding epoch is scored by clinical neurophysiologist as mild (blue), moderate (red) or severe (black). Two ellipsoids represent boundaries between classes as determined by quadratic classifiers. The larger one separates mild vs. moderate class, whereas the smaller

ellipsoid separates moderate vs. severe background EEG class. All data points are used only for training purposes, that is, to illustrate corresponding correlation between *dIBI* and visually scored background EEG grades.

Figure 1
Click here to download high resolution image

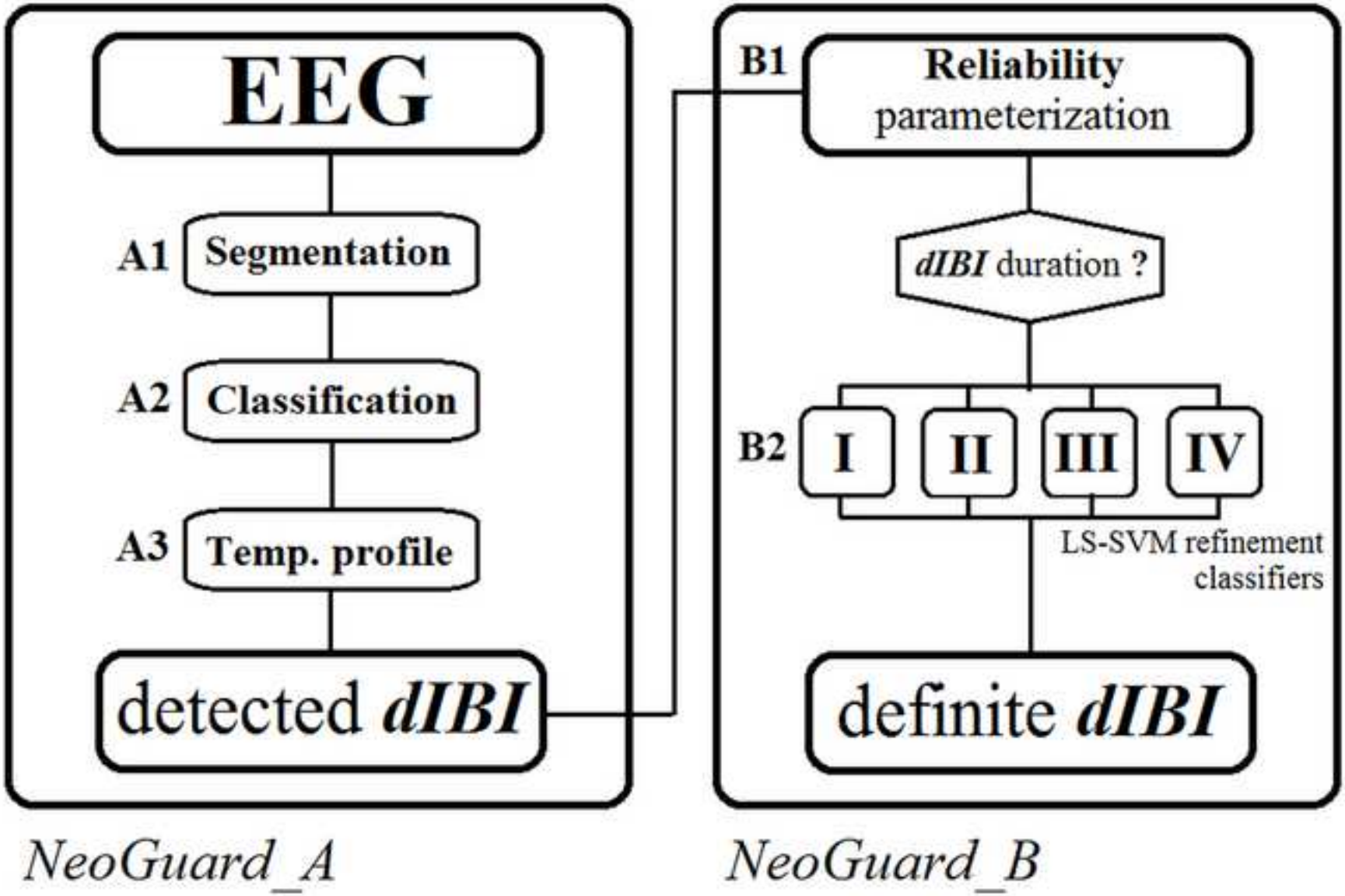


Figure 2

Click here to download high resolution image

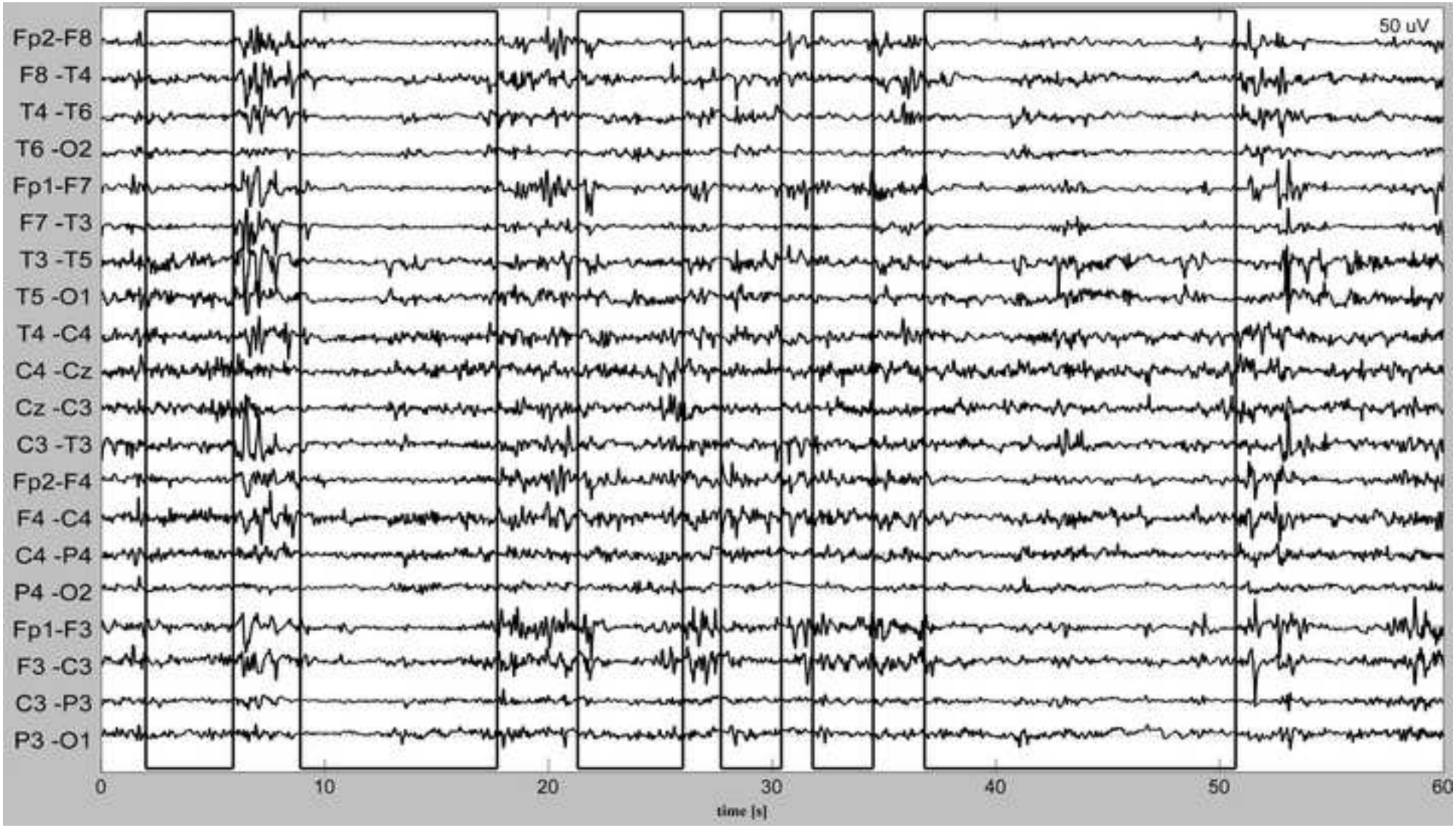


Figure 3

Click here to download high resolution image

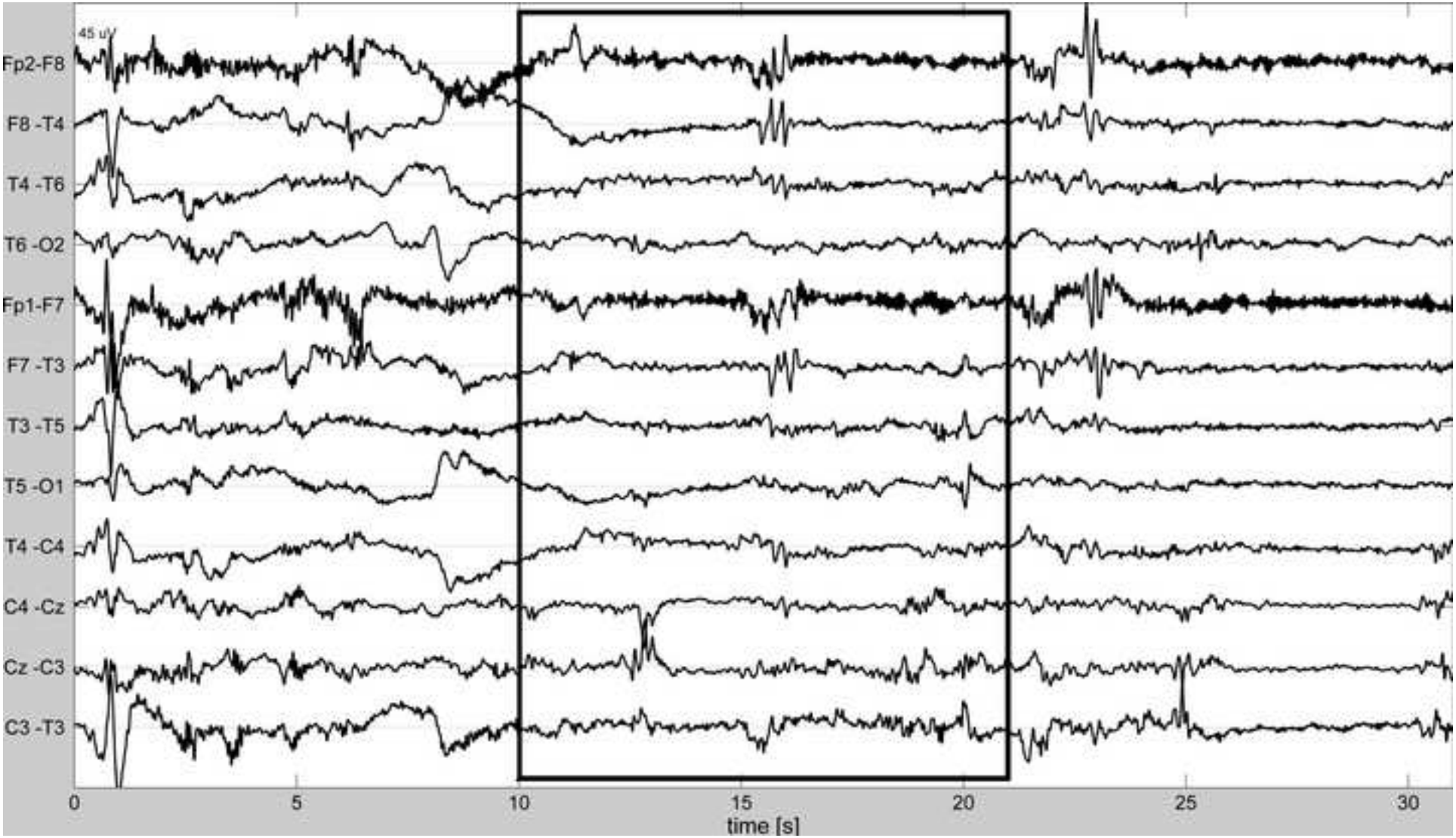


Figure 4

Click here to download high resolution image

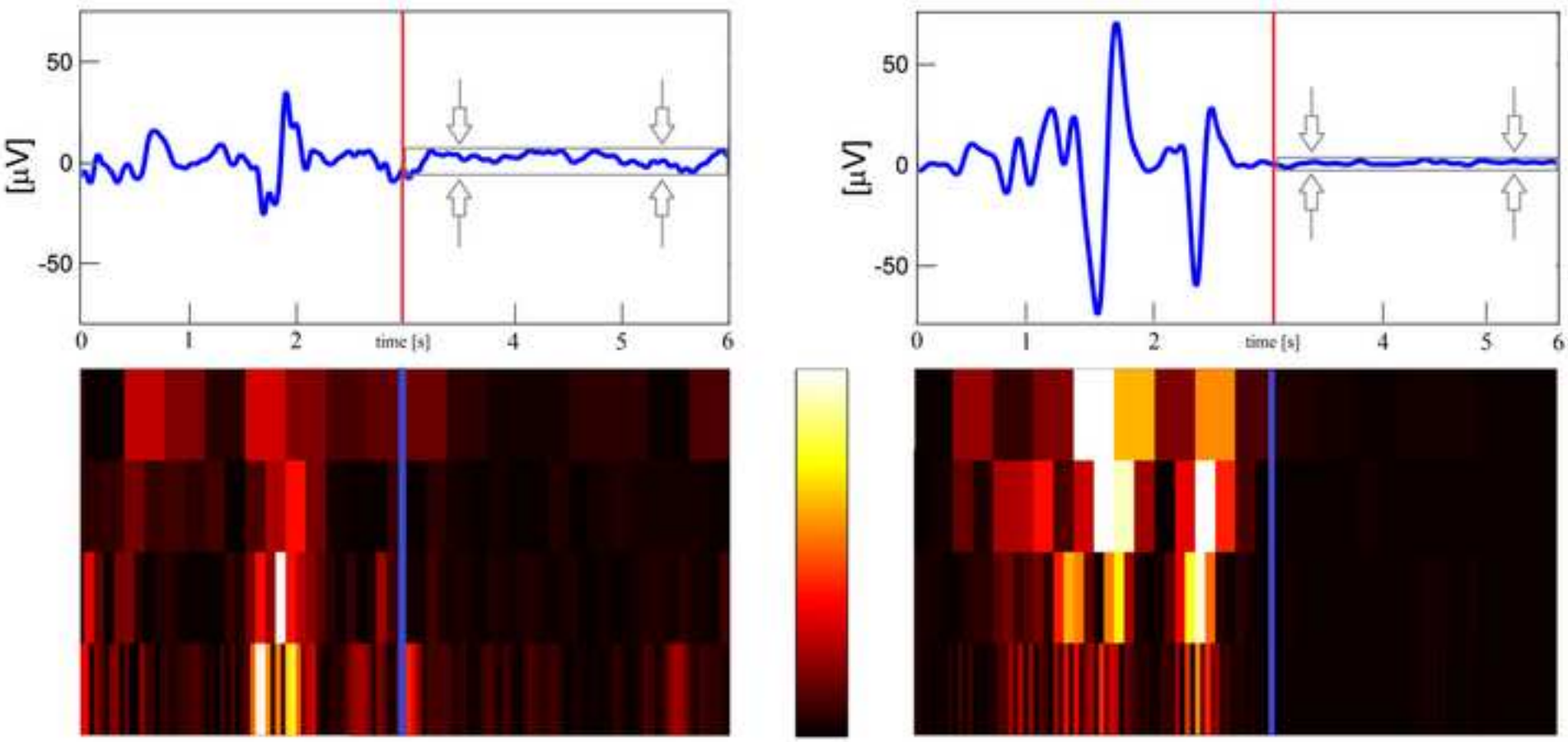


Figure 5a

Click here to download high resolution image

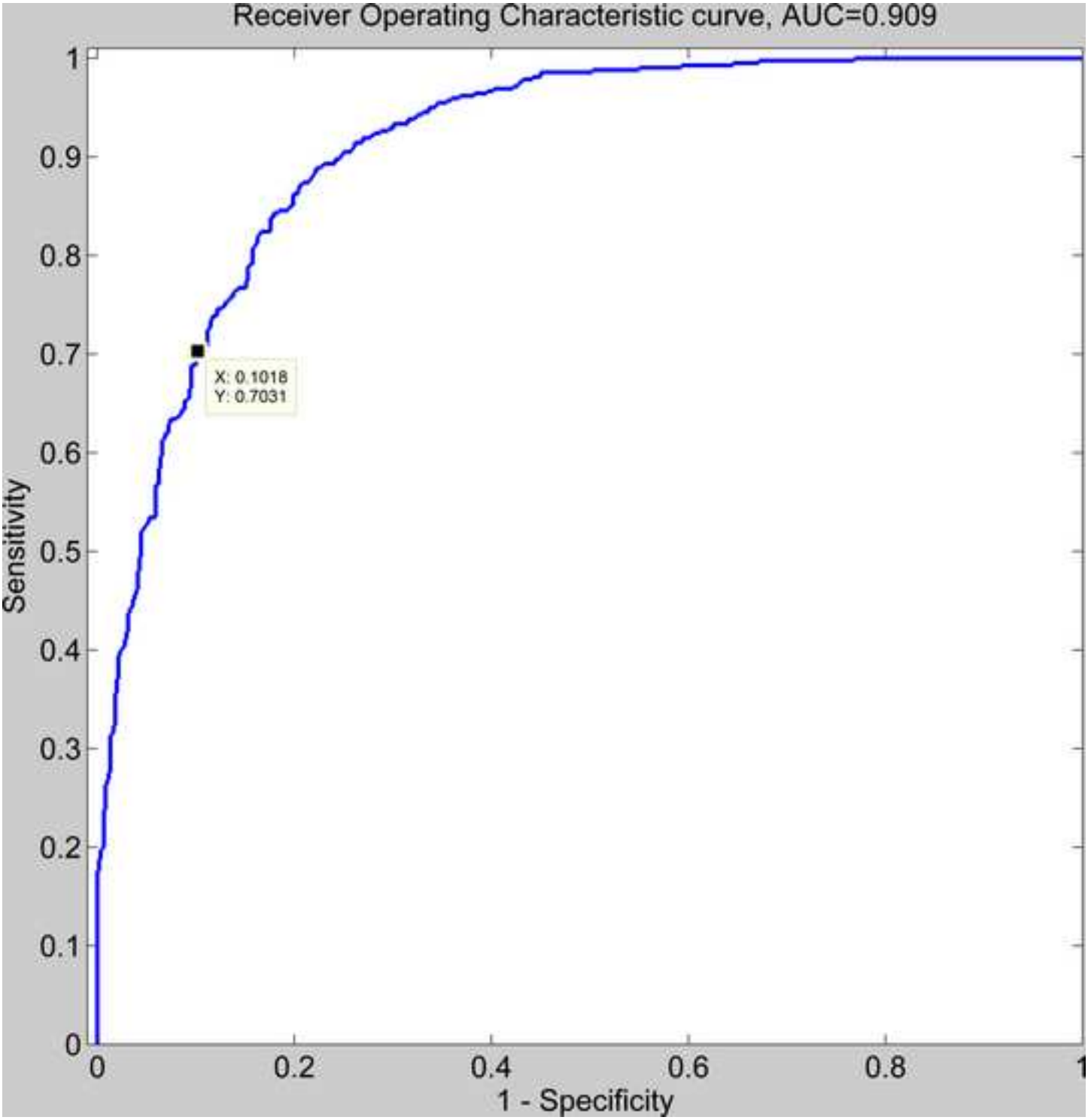


Figure 5b

Click here to download high resolution image

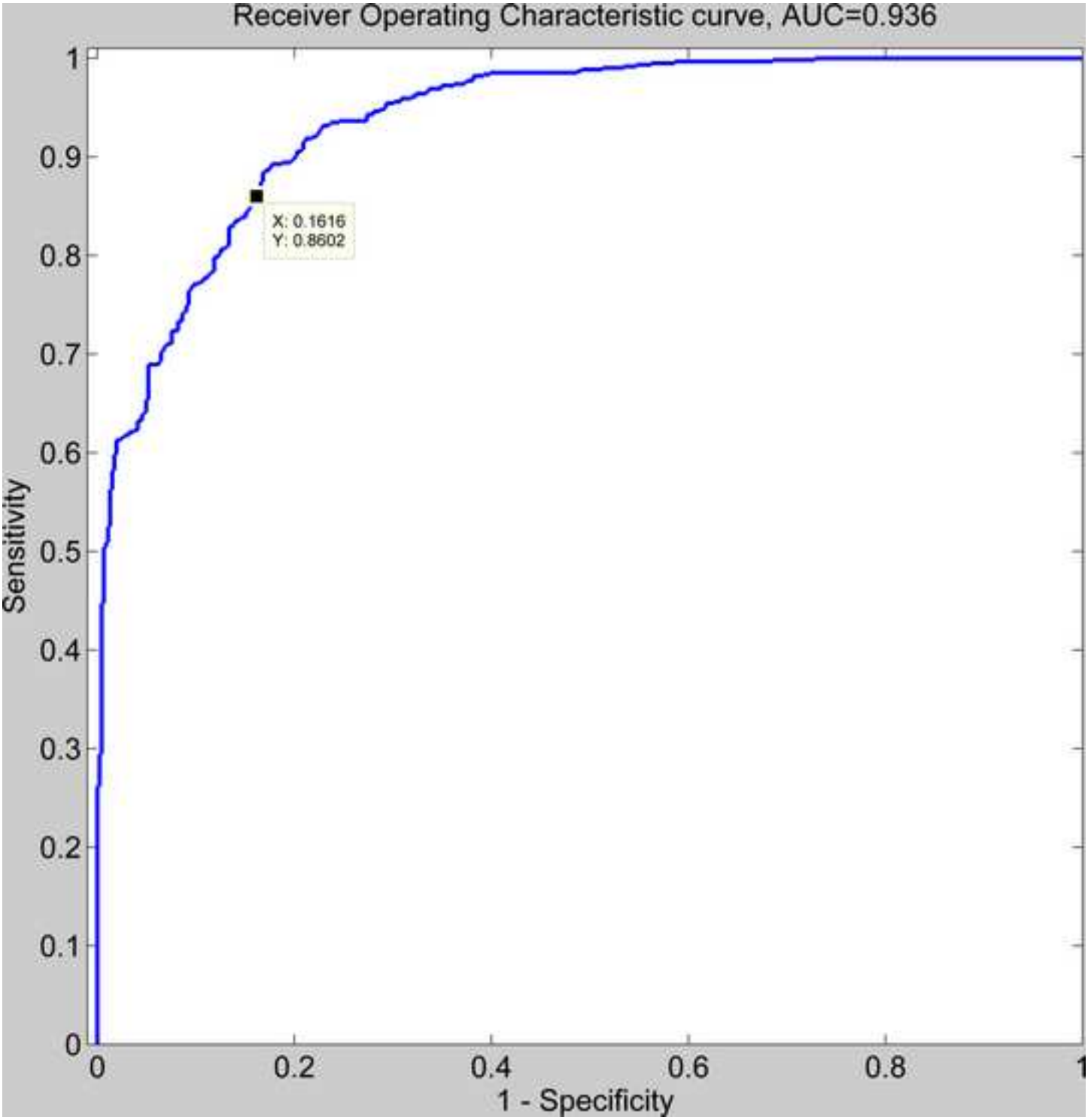


Figure 5c

Click here to download high resolution image

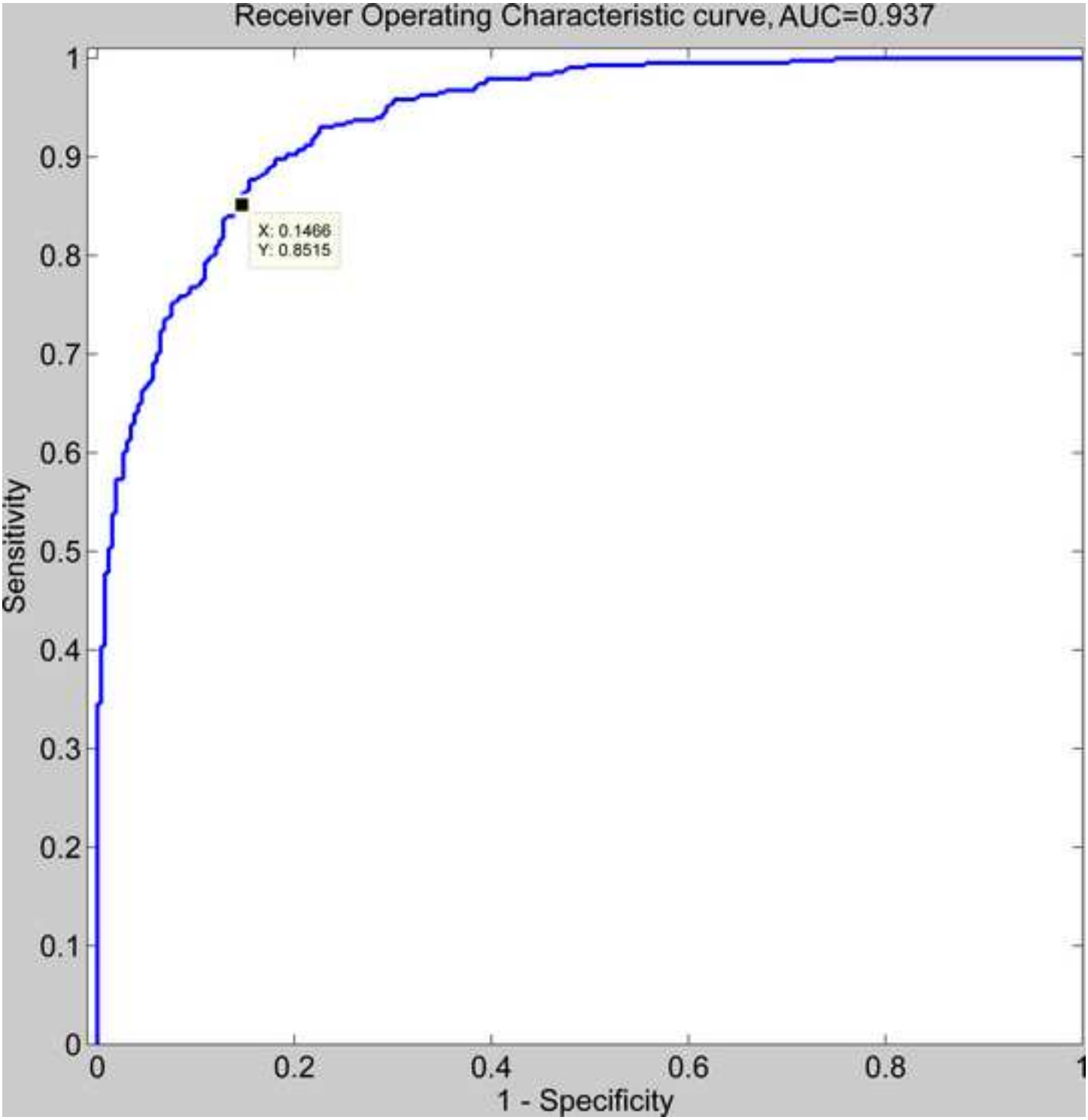


Figure 5d

Click here to download high resolution image

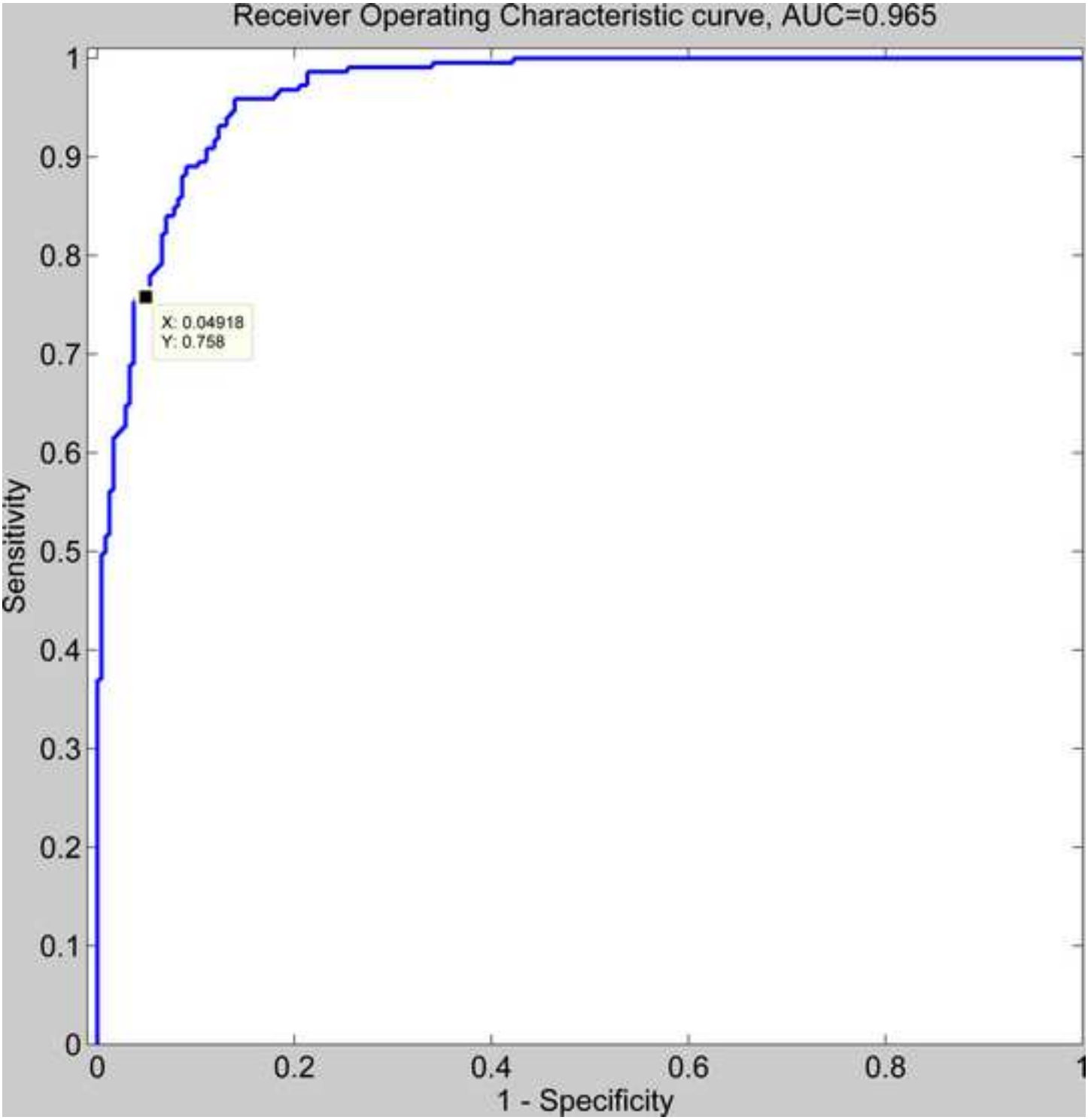


Figure 6
Click here to download high resolution image

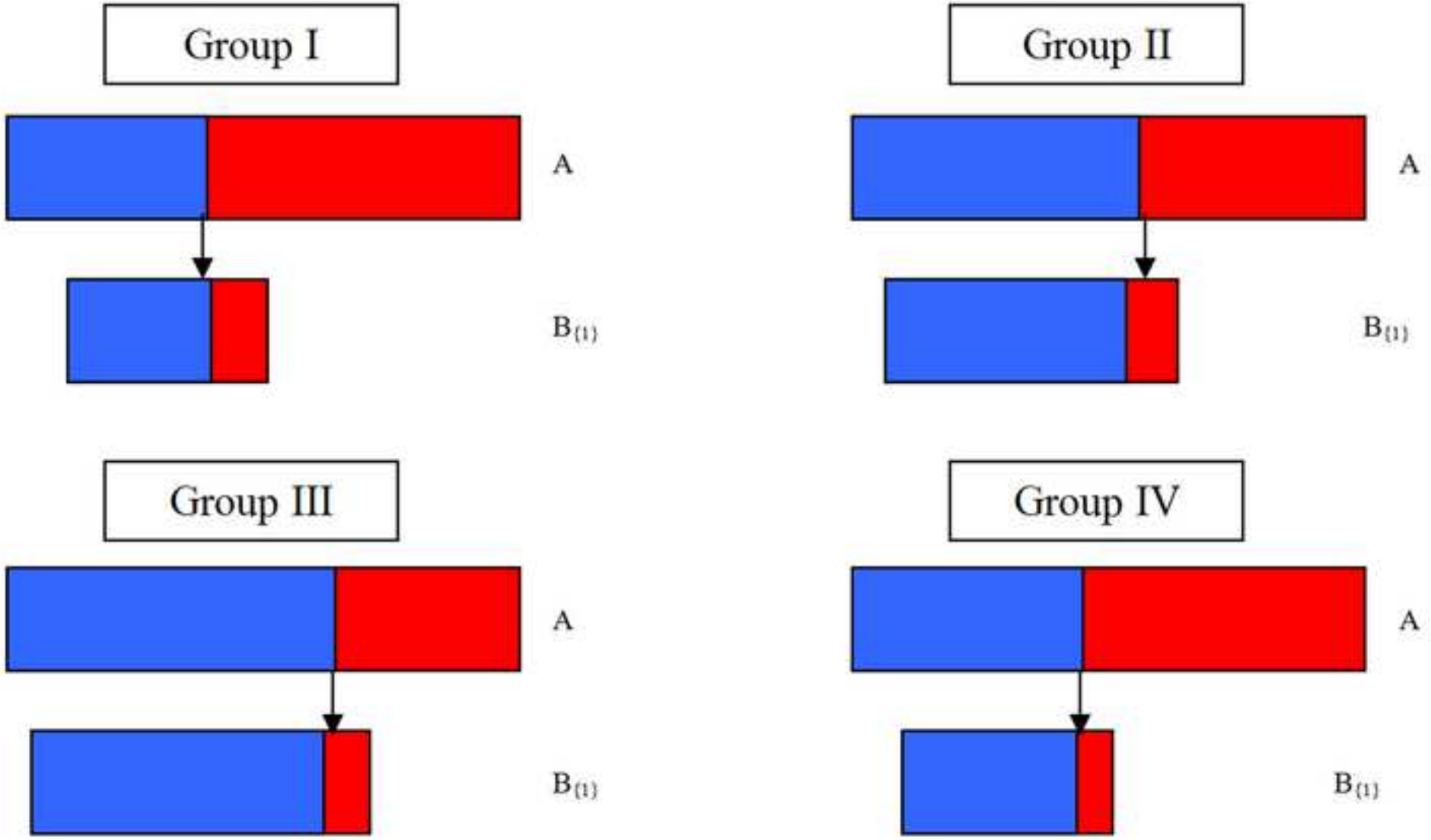


Figure 7

Click here to download high resolution image

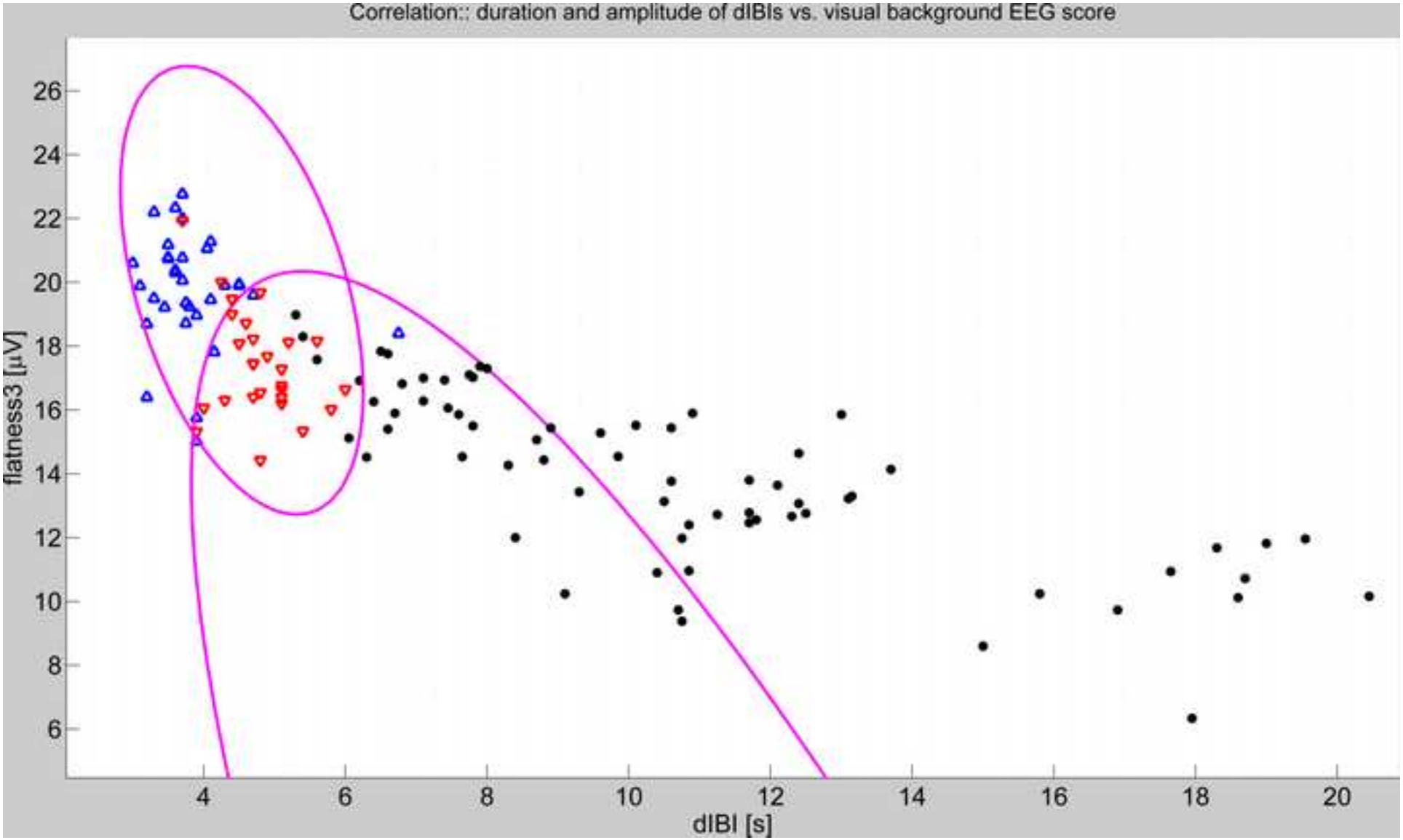


Table 1

dIBI duration group	*dIBI* duration [s]		Number of analyzed *dIBIs* detected by algorithm A
	From (≥)	To (<)	
I	3	5	1239
II	5	10	1382
III	10	20	881
IV	20	(>) 60	906

Table 1. Grouping of the *dIBIs* is derived from the *dynamic* interburst interval definition (Matic et al., 2013a, companion paper). In the last column, the number of *dIBIs* (total=4408), used for training and testing of the LS-SVM classifiers, is presented for each *dIBI* duration group.

Table 2

Table 2. Number of *dIBIs* detected in dataset DC using only algorithm A is presented in the 2nd column, whereas in the 3rd column number of definite *dIBIs* is shown as scored by an expert EEG reader (KJ). Next, the number (percentage) of kept *dIBIs* within the subset $B_{\{1\}}$ after the refinement step (using algorithm B, which excluded misclassified *dIBIs*) is presented in the 4th column. Finally, the number (percentage) of the accurately detected, *definite dIBIs* as confirmed by visual rater is shown.

dIBI duration group	Total number of detected *dIBIs* using algorithm A (N=835)	Number of *dIBIs* in subset $A_{\{1\}}$ marked by visual rater as *definite dIBIs*	Number of *definite dIBIs* within the reliable subset $B_{\{1\}}$ after the refinement step	Correctly detected *dIBIs* within the subset $B_{\{1\}}$ previously validated by the visual rater
I	280	189	128 (67%)	125 (98%)
II	330	254	209 (82%)	202 (97%)
III	169	126	102 (81%)	90 (88%)
IV	56	32	20 (63%)	19 (95%)

Author Agreement

Click here to download high resolution image

AUTHOR CONCURRENCE FORM

CLINICAL NEUROPHYSIOLOGY

Official Organ of the International Federation of Clinical Neurophysiology

http://www.elsevier.com/clinph

Prof. David Burke
Editor-in-Chief

Instructions:

1. Each submission to Clinical Neurophysiology needs a filled out Author Concurrence Form. Please fill in the Title of the manuscript.
2. Collect signatures from all authors.
3a. Scan the form and submit it together with the paper. The submission item is Author Agreement.
3b. If this is not an option, please fax the form to the Editorial Office: +31-20-485-3881.

Title of the Manuscript: Improving the reliability of automatically detected dynamic inter burst intervals in neonates with hypoxic ischemic encephalopathy

A signature below certifies compliance with the following statements.

Copyright Transfer: In consideration of the acceptance of the above manuscript for publication, the copyright is transferred to IFCN and administered by Elsevier. All proprietary rights other than copyright (such as patent rights) are reserved to the author, as well as the right to use original figures and tables in future works, provided full credit is given to the original publication. If the manuscript is work prepared by employee(s) of the United Kingdom or the United States government as part of their official duties, copyright cannot be fully transferred to the IFCN, and authors must check the appropriate box below.

- This manuscript was written in the course of employment by the United Kingdom and it is subject to Crown copyright.
- This manuscript was written in the course of employment by the United States Government and it is not subject to copyright in the United States.

Authorship Responsibility:

The submission is a truthful, original work without fabrication, fraud or plagiarism, and contains no libellous or unlawful statements.

It has not been published previously except in abstract form.

The manuscript is not under consideration for publication, nor will it be submitted for publication, elsewhere until a final decision has been made by this journal.

The undersigned certify that each has participated sufficiently in the work to take responsibility for its truthfulness and validity and has read the complete manuscript.

Conflict of interest disclosure:

All funding sources supporting this work are acknowledged. The authors will disclose to the editor any pertinent financial interests associated with the manufacture of any drug or product described in this manuscript.

ALL AUTHORS MUST SIGN

Vladimir Matic		Date 28.04.2013.
Perumpillichira J Cherian		Date 11.04.2013
Katrien Jansen		Date 19.04.2013
Ninah Koolen		Date 24.04.2013
Gunnar Naulaers		Date 24-04-2013
Renate M Swarte		Date 11.04.2013
Paul Govaert		Date 11.04.2013
Sabine Van Huffel		Date 29.04.2013
Maarten De Vos		Date 18-04-2013